



ParCFD2022

**PARALLEL COMPUTATIONAL  
FLUID DYNAMIC**

May 25th-27th 2022

Alba, Italy

[parcfd2022.org](http://parcfd2022.org)

[parcfd2022@sftc.ac.uk](mailto:parcfd2022@sftc.ac.uk)

**E4**

COMPUTER  
ENGINEERING



[www.e4company.com](http://www.e4company.com)

# An Efficient Parallel Solver for LES-DEM Simulation of Fluidized Bed

Fatima Ez-Zahra El Hamra<sup>\*</sup>, Aimad Er-raiy<sup>†</sup>, Radouan Boukharfane<sup>\*</sup>

<sup>\*</sup> Mohammed VI Polytechnic University (UM6P), MSDA Group, Benguerir, Morocco

<sup>†</sup> King Abdullah University of Science and Technology (KAUST), ECRC, Thuwal, KSA



# Contents

1. RESEARCH CONTEXT
2. DEM-LES FOR FLUIDIZED BED
3. PARALLELISM MANAGEMENT
4. SMALL SCALE BUBBLING FLUIDIZED BED
5. PARALLEL PERFORMANCE
6. CONCLUSION AND PERSPECTIVES

Research context



## Context and objectives



### Particle-laden flows are omnipresent...

→ Industry: biomass combustion, chemical industry, pharmaceutical, ...

→ Research: study of sedimentation, snow avalanche, and rheology.



### ... and still raise numerous questions

→ Experiments: measurement implementation.

→ Scale-up from lab-scale to industrial scale is a troublesome endeavor<sup>1</sup>.



## Objectives of the present study

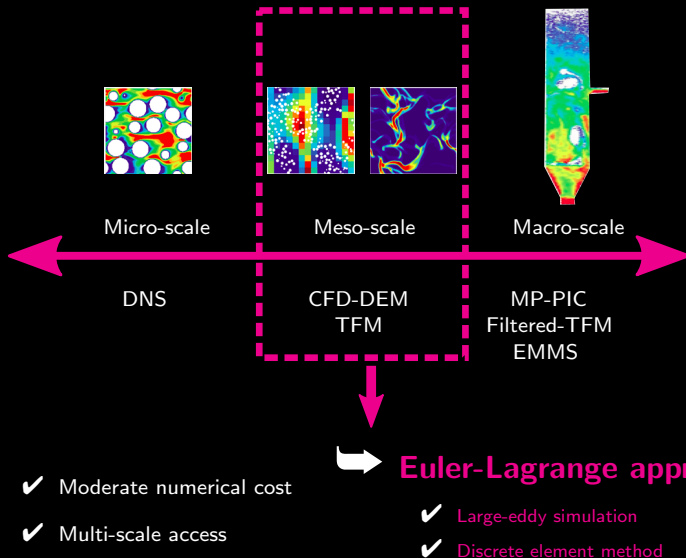
- Develop Parallel Eulerian–Lagrangian solver for 3D simulation of fluidized bed.
- Assess CFD-DEM capability to predict the instantaneous motion of particles.

<sup>1</sup> Rüdisüli, M., Schildhauer, T. J., Biollaz, S. M., & van Ommen, J. R. (2012). Scale-up of bubbling fluidized bed reactors—A review. Powder Technology, 217, 21–38.

**DEM–LES for fluidized bed**



# Fluidized bed: A numerical problem



# Discrete-element method (DEM)

## ➡ Newton's second law

$$\left\{ \begin{array}{l} m_p \frac{d\mathbf{u}_{p,i}}{dt} = \mathbf{f}_{p,i}^{\text{inter}} + \mathbf{f}_{p,i}^{\text{col}} + m_p \mathbf{g}_i, \text{ with } \frac{d\mathbf{x}_{p,i}}{dt} = \mathbf{u}_{p,i} \end{array} \right. \quad (1a)$$

$$\left\{ \begin{array}{l} \mathcal{F}_p \frac{d\boldsymbol{\omega}_{p,i}}{dt} = \mathcal{M}_{p,i}^{\text{drag}} + \mathcal{M}_{p,i}^{\text{col}} \end{array} \right. \quad (1b)$$

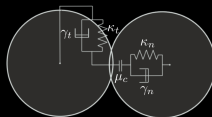
$$\mathbf{f}_{p,i}^{\text{inter}} \approx \gamma_p \partial_j \tau_{ij} + \mathbf{f}_{p,i}^{\text{drag}} \approx -\gamma_p \partial_i p^{\odot} + \mathbf{f}_{p,i}^{\text{drag}}$$

- Particle mass  $m_p = \pi \rho_p d_p^3 / 6$
- Particle-particle and particle-wall repulsion force  $\mathbf{f}_p^{\text{col}}$
- Force exerted on a single particle  $p$  by the surrounding fluid  $\mathbf{f}_p^{\text{inter}}$
- Drag and collision moments  $\mathcal{M}_{p,i}^{\text{drag}}$  and  $\mathcal{M}_{p,i}^{\text{col}}$

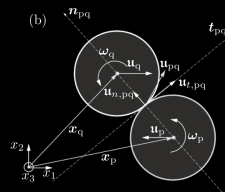
## ➡ Collision modelling

- ✓ Particle-particle and particle-wall collisions are modeled using the **Adaptive Collision Time Model (ACTM)**<sup>2</sup>

(a)



(b)



# Large-eddy simulation (LES)

## ➡ Filtered NS equations

$$\begin{cases} \partial_t (\theta_f \bar{\varrho}_f) + \partial_i (\theta_f \bar{\varrho}_f \widetilde{u_{f,i}}) = 0, \\ \partial_t (\theta_f \bar{\varrho}_f \widetilde{u_{f,i}}) + \partial_j (\theta_f \bar{\varrho}_f \widetilde{u_{f,i}} \widetilde{u_{f,j}}) = -\partial_j \bar{p} + \end{cases} \quad (2a)$$

$$\partial_j (\bar{\tau}_{ij} + \bar{\tau}_{ij}^{\text{SGS}}) + \theta_f \bar{\varrho}_f g_i + \mathcal{F}_i^{\text{inter}} \quad (2b)$$

$$\mathcal{F}^{\text{inter}} = \sum_{p=1}^{N_p} \xi(|\mathbf{x} - \mathbf{x}_p|) \mathbf{f}_p^{\text{inter}}$$

- where  $\theta_f$ ,  $\varrho_f$ , and  $\mathbf{u}_f$  are the fluid-phase volume fraction, density, and velocity, respectively.
- The force  $\mathbf{f}_p^{\text{inter}}$  exerted on a single particle  $p$  by the surrounding fluid is related to the interphase exchange term

## ➡ Subgrid-scale modelling

- ✓ The volume-filtered stress tensor

$$\bar{\tau}_{ij} = \mu \left[ \partial_i \overline{u_{f,j}} + \partial_j \overline{u_{f,i}} - \frac{2}{3} \partial_i \overline{u_{f,i}} \delta_{ij} \right] + \mathcal{R}_{\mu,ij}$$

- ✓ Effective viscosity  $\mu^*$  to account for enhanced dissipation

$$\mathcal{R}_{\mu,ij} \approx \mu^* \left[ \partial_i \overline{u_{f,j}} + \partial_j \overline{u_{f,i}} - \frac{2}{3} \partial_i \overline{u_{f,i}} \delta_{ij} \right]$$

- ✓ SGS eddy viscosity

$$\mu^{\text{SGS}} = \bar{\varrho} (C^{\text{SGS}} \Delta)^2 \sqrt{2 \bar{S}_{ij} \bar{S}_{ji}}$$

## Some Numerical details

- Projection method based on fractional time steps developed by Chorin <sup>3</sup> and improved by Kim & Moin <sup>4</sup>.
  - ✓ Fourth-order central scheme is used for the spatial integration
  - ✓ Third-order accurate semi-implicit Crank-Nicolson scheme is employed for time integration.
- Poisson equation is solved using the **Livermore's Hypre library** with the PCG (pre-conditioned conjugate gradient) method.
- The normalized drag force coefficients  $\mathbb{F}$  are modeled using **Tenneti's model** <sup>5</sup>

$$\mathbb{F}^{\text{TENNETI}}(\theta_f, \text{Re}_p) = \mathbb{F}^{\text{WY}}(\theta_f, \text{Re}_p) \theta_f^{1.65} + \theta_f \mathbb{F}_1^{\text{TENNETI}}(\theta_f) + \theta_f \mathbb{F}_2^{\text{TENNETI}}(\theta_f, \text{Re}_p)$$

with

$$\begin{cases} \mathbb{F}_1^{\text{TENNETI}}(\theta_f) = \frac{5.81(1-\theta_f)}{\theta_f^3} + \frac{0.48(1-\theta_f)^{1/3}}{\theta_f^4} \\ \mathbb{F}_2^{\text{TENNETI}}(\theta_f, \text{Re}_p) = (1-\theta_f)^3 \text{Re}_p \left[ 0.95 + \frac{0.61(1-\theta_f)^3}{\theta_f^3} \right] \end{cases}$$

<sup>3</sup> Chorin, A. J. (1968). Numerical solution of the Navier-Stokes equations. *Mathematics of computation*, 22(104), 745-762.

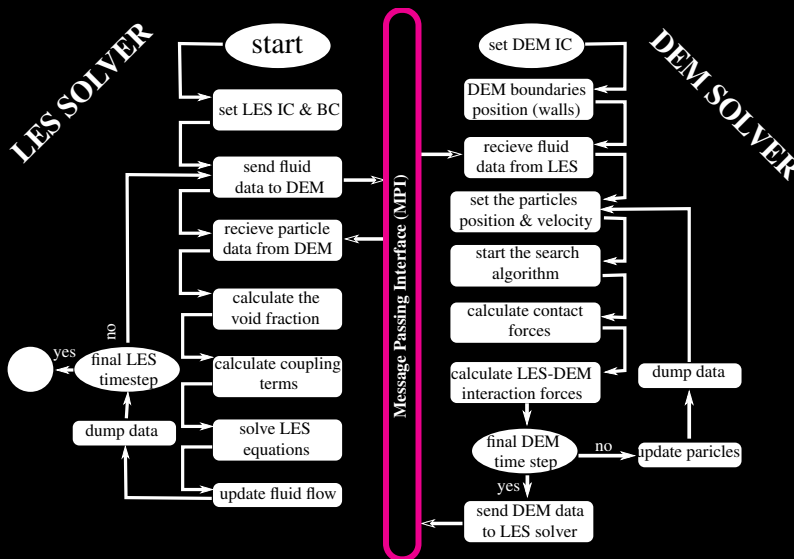
<sup>4</sup> Kim, J., & Moin, P. (1985). Application of a fractional-step method to incompressible Navier-Stokes equations. *Journal of computational physics*, 59(2), 308-323.

<sup>5</sup> Tenneti, S., Garg, R., & Subramaniam, S. (2011). Drag law for monodisperse gas-solid systems using particle-resolved direct numerical simulation of flow past fixed assemblies of spheres. *International journal of multiphase flow*, 37(9), 1072-1092.

## Parallelism management



# Parallelization strategy



## Parallelization strategy

➔ Schematic view of two-dimensional decomposition of particles with 4 processors

1D physical domain



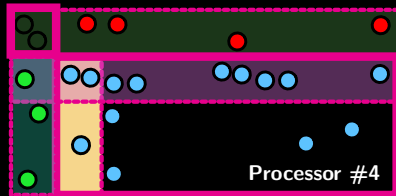
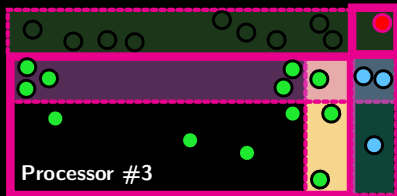
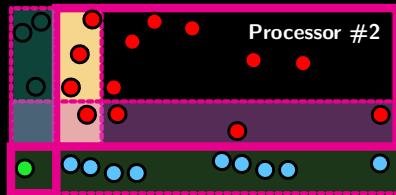
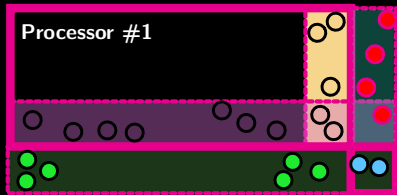
1D ghost domain



2D physical domain



2D ghost domain



## Parallel processing and data-structure update

```

begin
  Reconstruct: label Particle  $\mathbb{P}$ 
  hotpart false
  Create an empty list  $\mathcal{S}$ 
  if contour particle label changes at sub-domaine boundary then
    | activate particle as a hot particle; hotpart  $\leftarrow$  true
  end
  Ghost mappings: Particle
  if there is any hot ghost particle then
    | add it as a seed to the list  $\mathcal{S}$ 
  end
  Global: reduce operation on hotpart
  while hotpart do
    Reconstruct label Particle  $\mathbb{P}$  using flood fill from the seeds in  $\mathcal{S}$ 
    Empty:  $\mathcal{S}$ 
    Ghost mappings: Particle
    if there is any hot ghost particle then
      | add it as a seed to the list  $\mathcal{S}$ 
    end
  end
end
end
end

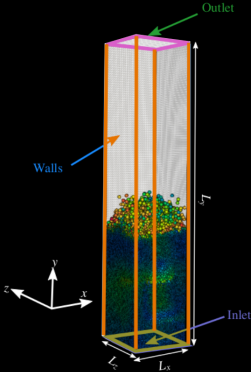
```

**Small scale bubbling fluidized bed**



# Small scale bubbling fluidized bed: Numerical setup

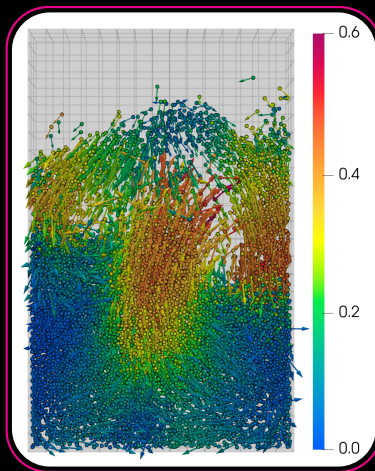
| Properties  | Müller <i>et al.</i> <sup>6</sup> | Van Wachem <i>et al.</i> <sup>7</sup> |
|---|-----------------------------------|---------------------------------------|
| Fluid phase   |                                   |                                       |
| Fluid density $\varrho_f$ [kg/m <sup>3</sup> ]                        | 1.2                               | 1.28                                  |
| Fluid viscosity $\mu$ [Pa·s]  | $1.8 \times 10^{-5}$              | $1.7 \times 10^{-5}$                  |
| Superficial gas velocity $u_\infty$ [m/s]                             | 0.6 – 0.9                         | 0.9                                   |
| Solid phase   |                                   |                                       |
| Number of particle  | 9240                              | 4080                                  |
| Particle diameter $d_p$ [mm]  | 1.20                              | 1.545                                 |
| Particle density $\varrho_p$ [kg/m <sup>3</sup> ]                     | 1000                              | 1150                                  |
| Inter-particle restitution coefficient $\epsilon_{dry}$               | 0.98                              | 0.90                                  |
| Particle-wall restitution coefficient $\epsilon_{dry}$                | 0.98                              | 0.90                                  |
| Inter-particle restitution coefficient $\mu_c$                        | 0.1                               | 0.3                                   |
| Particle-wall friction coefficient $\mu_c$                            | 0.1                               | 0.3                                   |
| Geometry and Mesh   |                                   |                                       |
| Bed $L_x \times L_y \times L_z$ [mm <sup>3</sup> ]                    | $44 \times 288 \times 10$         | $90 \times 450 \times 8$              |
| Grid number $\mathcal{N}_x \times \mathcal{N}_y \times \mathcal{N}_z$ | $16 \times 120 \times 4$          | $33 \times 168 \times 3$              |
| Non-dimensional parameters  |                                   |                                       |
| Particle Reynolds number $\mathcal{R}e_p$                             | 48, 72                            | 104.7                                 |
| Stokes number $St$  | 2.66 – 4                          | 5.81                                  |
| Archimedes number $Ar$  | $6.27 \times 10^4$                | $1.84 \times 10^5$                    |
| Galileo number $Ga$   | 250.41                            | 429.03                                |



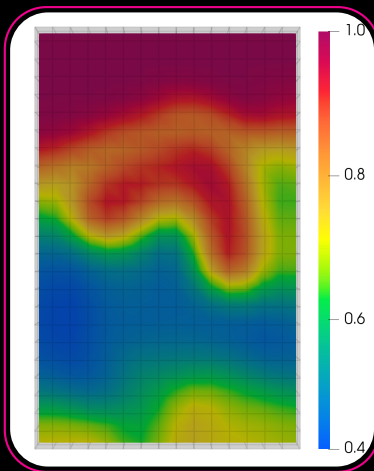
<sup>6</sup> Müller, C. R., Holland, D. J., Sederman, A. J., Scott, S. A., Dennis, J. S., & Gladden, L. F. (2008). Granular temperature: comparison of magnetic resonance measurements with discrete element model simulations. *Powder Technology*, 184(2), 241-253.

<sup>7</sup> Van Wachem, B. G. M., Van der Schaaf, J., Schouten, J. C., Krishna, R., & Van den Bleek, C. M. (2001). Experimental validation of Lagrangian–Eulerian simulations of fluidized beds. *Powder Technology*, 116(2-3), 155-165.

# Small scale bubbling fluidized bed: Qualitative analysis

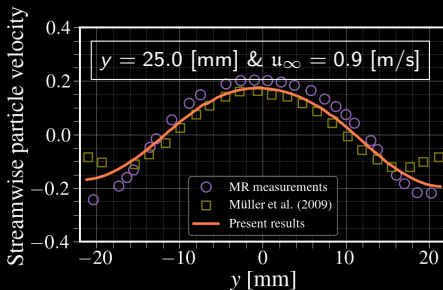
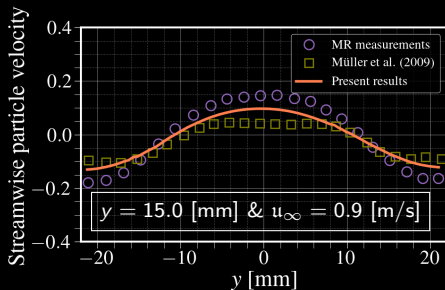
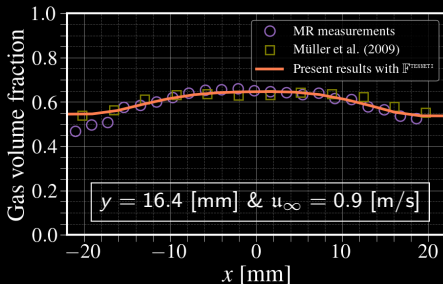
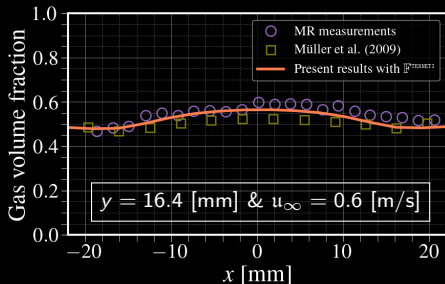


Instantaneous snapshots of the  
particle flow dynamic



a slice of the contours of the gas  
volume fraction

# Small scale bubbling fluidized bed: Quantitative analysis



**Parallel performance**

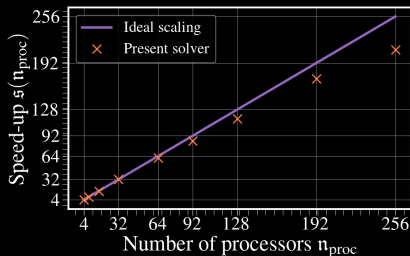


## Parallel performance on ASCC cluster

- A rectangular fluidized bed of 8 million particles and of dimensions  $0.1 \times 0.4 \times 0.1$  [m<sup>3</sup>].
- Uniform mesh is used with the cell size of 1.0 [mm], resulting in a total of 4 million cells in the LES grid.

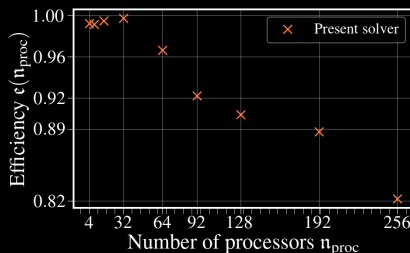
➡ Speedup factor

$$s(n_{\text{proc}}) = \frac{\text{Time}(\text{Serial})}{\text{Time}(n_{\text{proc}})}$$



➡ Efficiency

$$\epsilon(n_{\text{proc}}) = \frac{\text{Time}(\text{Serial})}{n_{\text{proc}} \text{Time}(n_{\text{proc}})}$$



## Conclusion and perspectives



# Few conclusions and many perspectives

## ● Conclusions

- ✓ A new solver coupling DEM and LES using parallelization strategies is developed.
- ✓ A thoroughly verification is performed.
- ✓ The results are agreeably compared with available measurements data.
- ✓ Good stability and high performance of the parallelization strategy.

## ● Perspectives

- ➔ Implementation of the particles feature complex geometries with a wide range of size distributions.
- ➔ Consideration of heat transfer model.
- ➔ Hybrid MPI/OpenMP or MPI/GPU framework.
- ➔ And so many other things to do ...

Thanks for tuning in!

Please leave comments & questions

Acknowledgments

African SuperComputing Center

